J Comput Aided Mol Des (2009) 23:153–162
DOI 10.1007/s10822-008-9247-y

Computational study on the molecular inclusion of andrographolide by cyclodextrin

Hongwei Zhou · Wai-Ping Lai · Zhiqiang Zhang · Wai-Kee Li · Hon-Yeung Cheung

Received: 17 May 2008 / Accepted: 18 September 2008 / Published online: 8 October 2008

Abstract Due to the poor water solubility of andrographolide (andro), an inclusion technique has been developed to modify its physical and chemical properties so as to improve its bioavailability. In contrast with the immense experimental studies on the inclusion complexes of andro:cyclodextrin, no computational study has so far been carried out on this system. In this work, preliminary docking experiments with AutoDock were performed. Density Functional Theory (DFT) and Austin Model 1 (AM1) calculations upon the docking instances were applied to investigate the two possible modes of molecular inclusions between andro and *x*-cyclodextrin (*x*CD, where *x* is α, β or γ). Atoms-in-Molecules (AIM) analysis based on the B3LYP/cc-pVDZ wavefunction was applied to verify the existence of the intermolecular hydrogen bonds. It was found that the most stable complex among the six possible inclusion complexes was the one formed between andro and βCD with andro's decalin ring moiety wrapped by CD at a ratio of 1:1. The hydrogen bonds between andro and CD were responsible for the stability of the inclusion complexes. The calculated data were found to be consistent with the experimental results. Thus, the results of this study can aid new drug design processes.

Electronic supplementary material The online version of this article (doi:10.1007/s10822-008-9247-y) contains supplementary material, which is available to authorized users.

H. Zhou · W.-P. Lai · Z. Zhang · H.-Y. Cheung (✉)
Research Group for Bioactive Products, Department of Biology and Chemistry, City University of Hong Kong, Kowloon, Hong Kong
e-mail: bhhonyun@cityu.edu.hk

W.-K. Li
Department of Chemistry, The Chinese University of Hong Kong, Shatin, NT, Hong Kong

Keywords Andrographolide · Cyclodextrin · Inclusion complex · Hydrogen bond

Introduction

Andrographolide (Fig. 1), or andro, the major constituent in the extract of *Andrographis paniculata* [1, 2], is known to possess a variety of pharmacological activities including analgesic, antipyretic and anti-inflammatory effects [3, 4]. Investigations on the cellular targets in human cancer [5, 6] and immune cells [7–10] after andro treatment indicate that andro is an important pharmacophore with anticancer and immunomodulatory activities. Hence, it is a promising cancer chemotherapeutic agent. However, andro is poorly soluble in water, and it is well known that the therapeutic efficacy of a drug, which is reflected by its bioavailability, is hampered by its poor solubility. In addition, andro is unstable towards oxygen. These disadvantages consequently limit the applications of andro. Research efforts to reveal the causes of poor therapeutic results and an array of methods to improve drug (including andrographolide) solubility have been attempted in recent years. Among the methods explored, the molecular inclusion technique is one of the most favorable approaches because it can significantly improve the solubility and prevent andro from hydrolysis in neutral or alkaline environments of the gastrointestinal tract [11, 12].

Cyclodextrins (CDs) are glucopyranosides, which are usually composed of 6–8 glucose units (Fig. 2). Topologically, CDs can be denoted as toroids with the smaller and the larger openings where some hydrophilic primary (at smaller opening) and secondary (at larger opening) hydroxyl groups are exposed to the outside of a toroid. Due to the special arrangement of functional groups, the interior

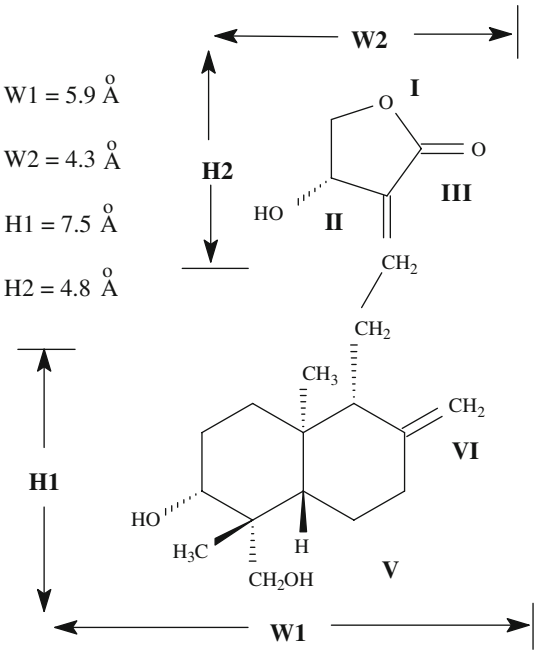

Fig. 1 Structure and sizes of the decalin ring moiety and the lactone moiety of andrographolide (andro)

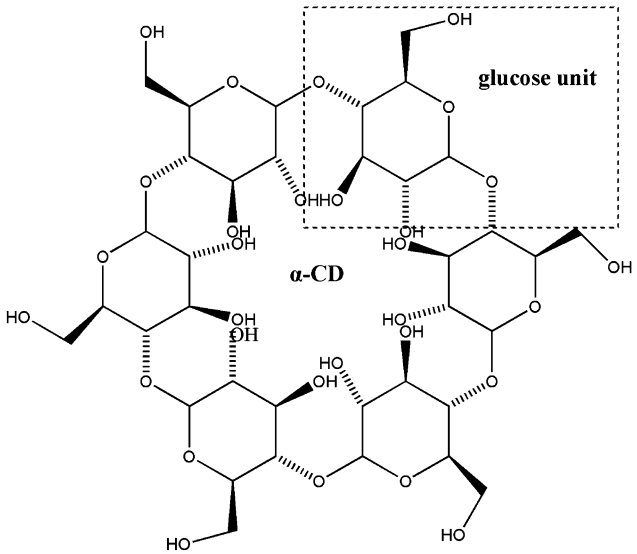

***α*CD**: 6 glucose units, ***β*CD**: 7 glucose units, ***γ*CD**: 8 glucose units.

Fig. 2 The sketch map of α-, β-, and γ-cyclodextrins (CDs)

of the toroid is considerably less hydrophilic than the aqueous environment. Thus, the cavity of CD is very suitable for other hydrophobic molecules to lodge inside. On the contrary, profiting from the existence of numerous "free" droxyl groups, the exterior of the toroid is sufficiently hydrophilic to render CDs (or their complexes) highly water-soluble. With these structural features, CDs are able to form host–guest complexes with hydrophobic molecules [13]. As a result of this function, CDs have applications in a wide range of fields. For example, in the environmental field, CDs can effectively immobilise toxic compounds inside their cavities to enhance the decomposition of these stable substances. In the food industry, the bulky and hydrophobic cholesterol molecule can easily be lodged inside CD toroid cavities that are then removed easily, leaving behind a low-fat food and reducing the unwanted tastes and odor. Perhaps CDs are particularly useful in pharmaceutics. A conveyer and carrier of drugs, CDs are often used to increase the solubility and stability and reduce the toxicity of some drugs [14]. Formation of inclusion complexes between CDs and a drug greatly modifies the physical and chemical properties, such as water solubility, of the guest molecule as well as the whole clathrates. Inclusion compounds of CDs with hydrophobic molecules can penetrate body tissues easily and then release biologically active compounds under specific conditions. Because of the non-covalent binding between CDs and the lodged molecules, the mechanism of controlled degradation of such complexes depends on the temperature and pH of water solutions, which can cause cleavage of hydrogen or ionic bonds between the host and the guest molecules. Furthermore, the α-1,4 linkages between glucose monomers of a CD can be cleaved by means of heating or action of the enzymes to disrupt the complexes and release the guest molecules.

Andro, as a guest molecule, could be easily encapsulated inside CD to form 1:1 or 1:2 inclusion complexes. Experimental results reported by Zhao et al. [11] and by us testified that the inclusion complex of andro:CD prefers a 1:1 molar ratio of a physical mixture of andro and CD. These 1:1 inclusion complexes have two isomeric forms: one has the decalin ring moiety of andro wrapped by CD, and another has the lactone moiety wrapped. However, which type of isomeric complexes is the predominant one has not yet been theoretically explained, though preliminary docking experiments and Fourier-transform infrared spectroscopy (FTIR) analysis provided some evidences that the predominant conformation is the decalin moiety of andro being encapsulated by CD (see electronic supplementary material—Table I, Fig. I). On the other hand, the main stabilizing factor of the inclusion complexes was supposed to be the hydrogen bonds (HBs) formed between andro and CD. However, these HBs have never been studied either experimentally or theoretically, due to the large structure and the complicated topology of the inclusion complexes. The present computational study on andro:CD complexes was an attempt towards this goal.

We have studied the bioactivity and bioavailability of this drug [8, 9] for some time. A promising molecular encapsulation technique has been developed to enhance the dissolution, bioavailability and stability of this drug. FTIR analysis of the inclusion complex showed that the

characteristic stretching bands of andro were significantly changed in inclusion complex, indicating that some important interactions (mainly hydrogen bonds) were taken place. Some other experimental results, such as the stabilities of the complexes, the drug releasing rates and drug dissolution efficiency are also the evidences of the existence of intermolecular interactions which need to be further identified and elucidated theoretically. Only parts of our results are listed in electronic supplementary material—Tables II and III. Details will be presented in our future report.

Computational methods

For the convenience of discussion, the complex in which the decalin ring moiety of andro encircled by CD was denoted as andro:*x*CD1 (where $x = \alpha, \beta, \gamma$), while the complex in which the lactone moiety of andro encircled by CD was referred to as andro:*x*CD2. Among the 10 species being investigated in this work, four were reference control molecules; i.e. andro, αCD, βCD and γCD. The remaining six were 1:1 inclusion complexes: andro:αCD1, andro:αCD2, andro:βCD1, andro:βCD2, andro:γCD1 and andro:γCD2. To obtain the rational conformations of the 1:1 inclusion complex, preliminary docking experiments with AutoDock [15–17] were performed to find where andro, as the ligand, interacts with or is docked into the CDs (as the macromolecule). Based on the predominant docking conformations, theoretical analysis was performed by carrying out full geometrical optimizations for the 10 species. The number of compounds, their size, and conformal flexibility make the geometrical optimization very expensive and difficult, precluding the use of more sophisticated ab initio methods such as Møller-Plesset or Hartree-Fock calculations, or even Density Functional Theory (DFT) calculations with large basis sets. Thus, all structures of the species were optimized using DFT with the small basis set STO-3G and using the economical Austin Model 1 (AM1) [18–21] method, followed by single-point calculations at the B3LYP/cc-pVDZ level using Gaussian 03 package [22].

Theoretically, two methods are commonly used to estimate the intra- or intermolecular HBs. One is the energy assessment, where the HB intensity can be measured by the energy differences between polymer and monomers. The other is the electron density assessment, where the HB intensity can be used to measure the spatial electron density of the region between two associated atoms. The former is very efficient if the precise energy is obtainable. However, for large-sized molecules or complexes, such as those in this work, it is difficult to obtain the precise energy of a complex. Hence we used the electron density assessment instead.

The electron distribution of a molecule is an excellent starting point to gain chemical insight into a molecule or an aggregate of molecules [23]. Since the interpretation of the charge density towards chemical concepts is essentially independent of the method by which the density is obtained, the charge density can be obtained from experiment or from a variety of computational schemes such as authentic density functional methods, e.g. Thomas-Fermi model and refinements [24], grid based methods [25] or the conventional SCF-LCAO-MO approach using any type of basis function. Among all known electron density methods, an appealing theory that takes advantage of this observation is the theory of "Atoms in Molecules" (AIM) [26–31]. Based on the charge density it partitions a molecular system into atoms in a natural way by using the concept of a gradient path. Integrating properties over these atomic basins is one of the cornerstones of AIM because it yields valuable information [32, 33]. For example, hydrogen bonding (both ordinary and exotic) can be confirmed solely from the charge density based on a handful of criteria, some of which invoke integrated atomic properties [34]. This is the reason why we have chosen the AIM theory to study the intramolecular HBs of the complexes in this work.

The topological properties of HBs in the complex were characterized using the AIM theory of Bader [26–31] with the AIM 2000 program package [35]. The AIM approach provides a rigorous procedure based upon the topology of density $\rho(r)$ to partition the molecule into atomic fragments Ω bound by a zero flux surface for the gradient vector field of $\rho(r)$. A crucial element of the theory is the set of properties of the critical points in $\rho(r)$, where $\nabla\rho$ vanishes. The points lying between bonded atoms are called bond critical points (BCPs). The BCP is a minimum of $\rho(r)$ along the bond path and a maximum in the interatomic surface. Local properties at BCPs convey valuable information about the molecular structure. The important element in this regard is the Laplacian of the density $\nabla^2\rho(r)$. Commonly, the $\nabla^2\rho$ identifies whether the charge of the region is locally depleted ($\nabla^2\rho > 0$) or concentrated ($\nabla^2\rho < 0$). The former is typically associated with interactions between closed-shell systems (ionic bonds, hydrogen bonds, and van der Waals forces), whereas the latter characterizes covalent bonds, where the electron density concentrates in the internuclear region. Our study on the electronic topologies of the inclusion complexes was concentrated on the BCPs with positive $\nabla^2\rho$ ($\nabla^2\rho > 0$). The existence of HB can be estimated by an BCP with a positive $\nabla^2\rho$ (i.e. $\nabla^2\rho > 0$) and an order of magnitude hundredth (i.e. 10^{-2}) of ρ value.

In summary, the four isolated molecules and the six complexes were optimized using DFT and AM1 methods at first. Then AIM calculations were applied to verify the existence of HBs inside the complexes.

Results and discussions

Identification of the rational conformations of the complex

In the docking experiments, andro was chosen as the ligand, while αCD, βCD or γCD as the inclusion macromolecules. By adding the ligand to the three CDs, 10 docking conformation instances for each andro:CD pair could be formed (electronic supplementary material—Table IV). As a result, 30 docking conformation instances in the pattern of the decalin moiety of andro encapsulated into the cavity of the CDs were identified. The data of binding energies and docking energies of each complex present in the table reveal which spatial conformations in each complex pair are more favorable. Since the lowest binding and docking energies represent the favorable spatial conformation they were picked up for further studies in comparison to some complexes in the lactone moiety of andro that may be encapsulated by CDs.

Energies

The four monomers (andro, αCD, βCD and γCD) and six inclusion complexes (andro:αCD1, andro:αCD2, andro:βCD1, andro:βCD2, andro:γCD1 and andro:γCD2) were optimized at the theory level of B3LYP/STO-3G as well as using the AM1 method. The energies of the 10 species and the energy difference (ΔE) between the inclusion complex and its two constituent monomers are listed in Table 1. The energy obtained at the B3LYP/STO-3G theory level is referred to as DFT energy, and the energy obtained using AM1 method is referred to as AM1 energy in this work. It is noted that the six inclusion complexes are so large-sized and complex that their atoms cannot be clearly labeled in ichnography. So, the labels for the atoms in each complex are summarized in Table 2.

The energies of all the six involved complexes were lower than the energy sums of their two constituent monomers, indicating that the association of andro and CDs had formed stable complexes. There were three pairs of isomers among the six complexes; namely Andro:αCD1 and andro:αCD2, andro:βCD1 and andro:βCD2, andro:γCD1 and andro:γCD2. Upon examining the relative energies of the isomeric pairs, it was found that andro and αCD prefer to have the lactone moiety of andro encapsulated inside the cavity of CD, though the latter conformation instance was not found in our docking experiment. On the other hand, both the andro:βCD and andro:γCD pairs prefer to have the decalin ring moiety of andro encapsulated inside the cavity of CD.

The relative stabilities of andro:CD inclusion complex were measured by their ΔEs, which can be regarded as the interaction energies or stabilizing energies. The lower the ΔE, the more stable the inclusion complex. Among the six inclusion complexes, the ΔE of andro:βCD1 (Table 1) was the lowest, indicating that it was the most stable complex. The ΔE of andro:αCD1 was the highest, indicating that it was the least stable. Our calculated results indicate that, as a host molecule, βCD can better encapsulate andro than the

Table 1 The AM1 and DFT energies (in au) of the 10 species, the energy difference ΔE (in kcal mol^{-1}) between the inclusion complex and the two molecules which form the complex

Species	AM1 energy	Complex	AM1 energy	ΔE[a]
AM1				
Andro	−0.36274			
αCD	−2.26671	Andro:αCD1	−2.63451	−3.2
βCD	−2.64417	Andro:αCD2	−2.63657	−4.5
γCD	−3.01659	Andro:βCD1	−3.02940	−14.1
Andro + αCD	−2.62945	Andro:βCD2	−3.01665	−6.1
Andro + βCD	−3.00691	Andro:γCD1	−3.39717	−11.2
Andro + γCD	−3.37933	Andro:γCD2	−3.39427	−9.4
DFT				
Andro	−1141.64670			
αCD	−3616.31601	Andro:αCD1	−4757.97595	−8.3
βCD	−4219.03841	Andro:αCD2	−4757.97661	−8.7
γCD	−4821.73836	Andro:βCD1	−5360.71496	−18.7
Andro + αCD	−4757.96270	Andro:βCD2	−5360.70472	−12.3
Andro + βCD	−5360.68511	Andro:γCD1	−5963.41219	−17.0
Andro + γCD	−5963.38506	Andro:γCD2	−5963.41026	−15.8

[a] $\Delta E = E_{complex} - E_{CD} - E_{Andro}$

Table 2 The assignment of the atomic labeling in the complexes

	Andro:αCD1	Andro:αCD2	Andro:βCD1	Andro:βCD2	Andro:γCD1	Andro:γCD2
CD	1–126	1–126	26–172	1–147	1–168	1–168
Andro	127–181	127–181	1–25, 173–202	148–202	169–223	169–223

α- and γ-CDs. This is why βCD is commonly chosen as host molecule for andro in pharmacy [36–41].

As mentioned in the Introduction section, the three CDs can be topologically represented as toroids with the larger and the smaller openings of the toroid exposed to the secondary and primary hydroxyl groups of the solvent, respectively. Previous studies [11–14] have verified that the guest molecule insert into CD from the larger opening of the toroid instead of the smaller one. In fact, the docking display exhibits that andro was inserted into the cavity of the CDs from the larger opening in all the docking conformation instances. Hence, matching the diameters of the toroid with the maximum width of encapsulated moiety of andro plays an important role in the formation of a stable inclusion complex. The height and the inner diameters of the cavity in CDs are shown in Fig. 3. The height and the widths of the decalin ring moiety and the lactone moiety of andro are shown in Fig. 1. The inner diameters of the toroid of αCD range from 5.3 to 7.5 Å, while the width of decalin ring moiety is about 5.9 Å, and the width of the lactone moiety is about 4.3 Å. Hence in the andro:αCD1 inclusion complex, only a small portion of the decalin ring was wrapped. Docking display shows that the top 10 docking conformation instances of andro:αCD were in this form. As shown in Fig. 4, the decalin ring was deterred from entering the large opening of the αCD cone. In fact, only the methyl, methanol and hydroxyl groups on the decalin were wrapped by αCD. This type of inclusion complex was not very stable and had caused little modification of the physical and chemical properties of andro because only small part of andro was wrapped by αCD. In the andro:αCD2 inclusion complex, the whole lactone moiety entered the toroid of αCD, which made this inclusion complex more stable than andro:αCD1. As a result, andro's chemical properties were greatly modified. By contrast, βCD (6.3 Å for the small opening and 9.2 Å for

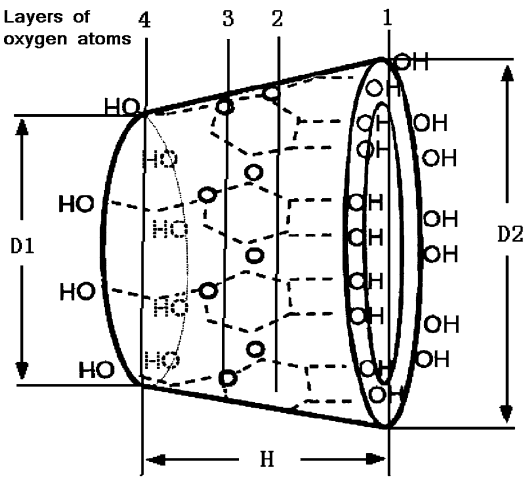

	D1	D2	H
αCD	5.3Å	7.5Å	5.0Å
βCD	6.3Å	9.2Å	5.0Å
γCD	7.2Å	11.0Å	5.0Å

Fig. 3 Showing of spatial arrangement of the glucose units in γCD toroid structure, and height and the inner diameters of the cavity in CDs

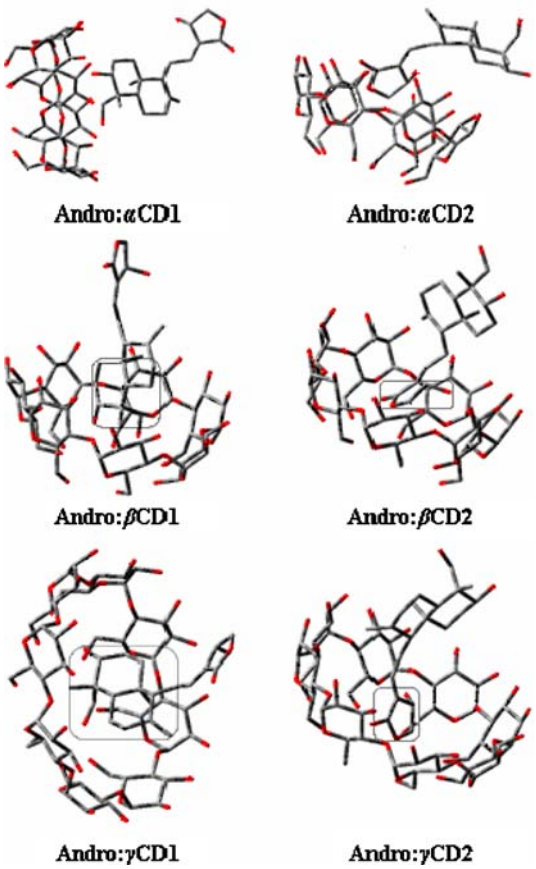

Fig. 4 Spatial arrangement of six possible inclusion complexes of andro:CD (1:1). The part bounded by a square is the moiety which is encapsulated by CD

the larger opening) and γCD (7.2 and 11.0 Å, respectively) wrapped both the decalin ring moiety and the lactone moiety of andro. Consequently, the physical and chemical properties of andro were modified and were dependant on the degree of encapsulation of andro. The percentage of the encapsulated part was larger with the decalin ring moiety being wrapped than that of the lactone moiety, as the former is physically larger than the latter. In other words, if andro enters inside the large opening of βCD with its decalin ring moiety, its physical and chemical properties undergo significant modification. The same situation holds for γCD. However, the cavity diameter of γCD is too large to retain andro, i.e., the interaction between the andro and the "hydrophobic" part inside of cavity of γCD is weaker than that formed between andro and βCD. Hence, andro:βCD should be more stable than andro:γCD.

HBs in the inclusion complexes

AIM calculations were carried out to investigate the HBs inside the six 1:1 andro:CD inclusion complexes. There were 231, 242, 282, 277, 298 and 297 BCPs in andro:αCD1, andro:αCD2, andro:βCD1, andro:βCD2, andro:γCD1 and andro:γCD2, respectively (Table 3). Among these BCPs, the BCPs with negative $\nabla^2\rho$ were identified as covalent bonds, while those with positive or zero $\nabla^2\rho$ were identified as HBs. The exception was the *C*=O bond, which clearly was a covalent bond, even though its $\nabla^2\rho$ was positive in AIM analysis. Thus, there were 42, 53, 71, 66, 65 and 65 HBs in andro:αCD1, andro:αCD2, andro:βCD1, andro:βCD2, andro:γCD1 and andro:γCD2, respectively. The bond path (BP) lengths, the electron densities (ρ) and the Laplacian of ρ ($\nabla^2\rho$) are provided in the electronic supplementary material (Tables V–X). The numbers of BCP in the complexes are listed in Table 3. Besides the "normal" HBs, which are in the form of X–H···Y, there existed considerable amounts of so-called "double" HBs, with the form of X–H···H, in the six inclusion complexes. Some were intermolecular HBs (hydrogen bonds between andro and CD), and some were intramolecular HBs (either inside CD or inside andro).

Among the numerous HBs in each inclusion complex, the intermolecular HBs, including the "normal" and "double" HBs, have the most influence towards the stability of the inclusion complex. The following discussion emphasizes on the "normal" intermolecular HBs in the inclusion complexes. For the convenience of discussion, in andro, the six oxygen atoms acting as proton acceptors of intermolecular HB are labeled **I**, **II**, **III**, **IV**, **V** and **VI**, respectively (Figs. 1, 5). The proton donors (hydrogen atoms) are located at eight regions, which are bounded by rectangles, and denoted as ***a*–*h***, respectively in Fig. 5. In CD, the proton acceptors (oxygen atoms) can be divided into four layers. Starting from the larger opening, the layers are numbered as **1**, **2**, **3** and **4** (Figs. 3, 5). The oxygen atoms in layers **1** and **4** are in the form of hydroxyls. The oxygen atoms in layer **2** are the linking atoms between two glucopyranoside units, while the oxygen atoms in layer **3** are located inside the hexagon framework of glucopyranoside. The hydrogen atoms in CD could point either inwards or outwards from the cavity. Those pointings inwards can be divided into four layers similar to the oxygen atoms in the CD. Starting from the large opening side, the layers are numbered as **1**, **2**, **3** and **4** (Figs. 3, 5).

Table 3 Count of BCPs, covalent bonds and hydrogen bonds in the inclusion complexes

	BCP	CVB	HB	Normal HB			Double HB		
				Inter	CD	Andro	Inter	CD	Andro
Andro:αCD1	231	189	42	4	18	3	9	0	8
Andro:αCD2	242	189	53	10	20	3	11	0	9
Andro:βCD1	282	211	71	17	24	2	18	1	9
Andro:βCD2	277	211	66	14	24	3	13	0	12
Andro:γCD1	298	233	65	8	27	2	17	3	8
Andro:γCD2	297	233	65	13	26	3	12	1	9

BCP: The total number of bond critical points; CVB: the total number of BCP for covalent bonds; HB: the total number of BCP for hydrogen bonds; Normal HB: the number of HBs which have the form of X–H···Y; Double HB: the number of HBs which have the form of X–H···H; Inter: the number of HBs between andro and CD, i.e. intermolecular HBs; CD: the number of HBs inside CD, i.e. intramolecular HBs; Andro: the number HBs inside andro, i.e. intramolecular HBs

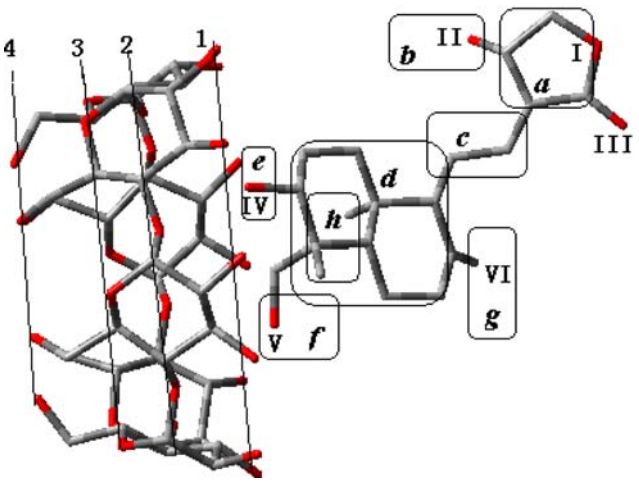

Fig. 5 Structure of andro:CD (1:1) inclusion complex. Numbers **1**, **2**, **3**, **4** denote the layers of proton acceptors or proton donors of CD. Roman numbers **I–IV** denote the proton acceptor (mainly oxygen atoms) atoms in andro. Rectangle denoted by ***a***, ***b***, ***c***, ***d***, ***e***, ***f***, ***g***, ***h*** represent the regions where proton donors are located

Table 4 The bond path length (BPL, in Å), electron density ρ and Laplacian $\nabla^2\rho$ of the bond critical points for intermolecular hydrogen bonds in the inclusion complex andro:αCD1

X	HB (BCP)	BPL	ρ	$\nabla^2\rho$	PPA	PPD
C142	H173···O63	2.393	0.013	0.036	**1**	***h***(C)
C134	H155···O65	2.717	0.007	0.021	**1**	***d***(C)
C131	H102···O132	2.262	0.016	0.040	**V**	**2**(C)
C128	H122···O127	2.318	0.013	0.039	**IV**	**2**(C)

X: X–H···Y; PPA: position of proton acceptor (carbon or oxygen atom), see text and Fig. 5; PPD: position of proton donor (hydrogen atom). The atom linked to the proton donor is in parentheses. The element in the parentheses is the donor

Intermolecular HBs in andro:αCD1

There are four intermolecular HBs in this inclusion complex (Table 4). The bond path length (BPL) is regarded as the approximate distance (usually slightly overestimated) of H···Y out of the X–H···Y formation. It can be found that the shortest BPL (2.262 Å) was H102···O132 of the C131–H102···O132 formation, with the largest ρ value (0.016), indicating that this HB was the strongest among the four HBs. The longest BPL (2.717 Å) was for H155···O132 of the C134–H155···O132 formation, with the smallest ρ value (0.007), indicating that this HB was the weakest HB among the four HBs. The proton acceptors of C142–H173···O63 and C133–H155···O65 come from layer **1** of CD, while the proton donor of C142–H173···O63 comes from the methyl group on the decalin ring (PPD = ***h*** in Table 4, PPD: position of proton donor) of the andro and that of C133–H155···O65 comes from the decalin ring (PPD = ***d*** in Table 4). The proton acceptor of C131–H102···O132 and C128–H122···O127 come from the methylol group (PPA = **V** in Table 4, PPD: position of proton acceptor) and the hydroxyl group (PPA = **IV** in Table 4) on the decalin ring of the andro, respectively, while the proton donors come from layer **2** of CD. Obviously, the atoms associated with proton donor are all carbon atoms, with electronegativity lower than that of oxygen. This type of HB is surely weaker than the normal HB in which the proton donor links to a highly electronegative atom, such as O, N, F etc. Thus the inclusion complex between andro and CD linked by this type of HB is not very stable.

Intermolecular HBs in andro:αCD2

There are 10 intermolecular HBs in this inclusion complex (Table 5). Among them, the proton acceptors are mainly the three oxygens in the lactone moiety of andro and the oxygens in layer **1** (in the form of hydroxyl) of CD. The proton acceptor of C128–H152···O18, i.e. O18, comes from layer **2**, while for C54–H112···C130, the proton acceptor is a carbon atom, C130, which forms a double bond (in region ***c*** of andro). The proton donors of these two HBs come from layers **2** and **3** of CD, or from the framework of the decalin of andro. Meanwhile, H152 of C128–H152···O18 comes from the framework of the lactone of andro. Similar to HBs in the andro:αCD1, the atoms associated to proton donor are all carbon atoms, indicating that they are not ideal HBs. There are two HBs associated with O127, which is in the lactone of andro, C34–H90···O127 and C45–H100···O127. Both have low ρ values and long BPLs, implying a weak intermolecular HB. In addition, O127 is also involved in another weak interaction, O29···O127 (region **I**), with a very low ρ value (0.003) and long BPL (3.436 Å).

Table 5 The bond path length (BPL, in Å), electron density ρ and Laplacian $\nabla^2\rho$ of the bond critical points for intermolecular hydrogen bonds in the inclusion complex andro:αCD2

X	HB (BCP)	BPL	ρ	$\nabla^2\rho$	PPA	PPD
C128	H152···O18	2.332	0.013	0.037	**2**	***a***(C)
C136	H159···O63	2.470	0.011	0.030	**1**	***d***(C)
C140	H166···O63	2.368	0.012	0.035	**1**	***d***(C)
C12	H72···O133	2.371	0.013	0.033	**II**	**2**(C)
C34	H90···O127	3.103	0.002	0.010	**I**	**3**(C)
C32	H92···O132	2.372	0.012	0.035	**III**	**2**(C)
C45	H100···O127	3.643	0.001	0.003	**I**	**3**(C)
C43	H102···O132	2.516	0.008	0.025	**III**	**2**(C)
C54	H112···C130	3.482	0.002	0.006	**c**	**2**(C)
	O127···O29	*3.436*	*0.003*	*0.014*	***I***	***2***

PPA and PPD: see the footnote of Table 4

An intermolecular interaction *O127…O29*, which is not a hydrogen bond because neither the proton donor nor the proton acceptor is a hydrogen atom, was found in this inclusion complex. It was listed here in italic only for reader's reference

Comparing these two andro:αCD inclusion complexes, andro:αCD2 has more intermolecular HBs and more layers (layers **1**, **2** and **3**) participating in the interactions than andro:αCD1, indicating that the andro:αCD2 inclusion complex is more stable. These results are consistent with the conclusion obtained based on the two ΔEs.

Intermolecular HBs in andro:βCD1

There are 17 intermolecular HBs in this inclusion complex (Table 6). Among them, the proton acceptors come from the functional group hydroxyl (region **IV** in Fig. 1 or 5) and methylol (**V** in Fig. 1 or 5) of the decalin ring moiety of andro, or from layers **2** or **4** of the CD. The proton donors come from layers **3** or **4** of the CD, or from the regions ***d***, ***e***, ***f*** and ***h***, all of which are in the decalin moiety of andro. There are six typical HBs with proton donors connecting with highly electronegative oxygen

Table 6 The bond path length (BPL, in Å), electron density ρ and Laplacian $\nabla^2\rho$ of the bond critical points for intermolecular hydrogen bonds in the inclusion complex andro:βCD1

X	HB (BCP)	BPL	ρ	$\nabla^2\rho$	PPA	PPD
O100	H110···O18	2.41	0.01	0.038	**IV**	**4**(O)
C28	H155···O18	2.55	0.009	0.028	**IV**	**3**(C)
C40	H165···O18	2.421	0.011	0.034	**IV**	**3**(C)
O43	H170···O18	2.436	0.011	0.043	**IV**	**4**(O)
C88	H115···O21	2.262	0.016	0.044	**V**	**3**(C)
O95	H120···O21	2.542	0.009	0.038	**V**	**4**(O)
C77	H125···O21	2.986	0.003	0.015	**V**	**3**(C)
O84	H130···O21	2.198	0.015	0.049	**V**	**4**(O)
O18	H178···O26	2.161	0.018	0.056	**4**	***e***(O)
C15	H176···O34	2.386	0.011	0.034	**2**	***d***(C)
C15	H175···O44	2.784	0.005	0.020	**2**	***d***(C)
C16	H177···O52	3.015	0.003	0.013	**2**	***d***(C)
C19	H179···O63	2.801	0.005	0.020	**2**	***h***(C)
C19	H180···O74	2.797	0.005	0.019	**2**	***h***(C)
C20	H182···O85	2.655	0.007	0.023	**2**	***f***(C)
C20	H183···O96	2.763	0.006	0.022	**2**	***f***(C)
O21	H184···O100	2.192	0.016	0.045	**4**	***f***(O)

PPA and PPD: see the footnote of Table 4

atoms. These six HBs have high ρ values (e.g. 0.018 for O18–H178···O26) and short BPLs (e.g. 2.161 Å for O18–H178···O26). The proton donors of the remaining eleven HBs involve the less electronegative carbon atoms. In general, O–H···O HBs are stronger than C–H···O HBs, from the consideration of ρ values or BPLs.

Viewed from the topology of the inclusion complex, it can be found that the atoms on decalin interact with mainly the atoms in the middle layers (layers **2** and **3**, where the "hydrophobic" regions inside the cavity are located) of the CD to form the corresponding HBs. Specifically, the seven "bridge" oxygen atoms (which is the linking atom between two glucopyranoside units) and the hydrogen atoms in decalin ring form seven HBs. The midsection of the cavity of CD is relative "hydrophobic". This arrangement of HBs, on one hand, renders the inclusion complex to be stable. On the other hand, the relative "hydrophilic" parts of CD, that is, the layers **1** and **4** (all are hydroxyl groups) are preserved for dissolution in water. Hence, andro:βCD1 is an ideal inclusion complex.

Intermolecular HBs in andro:βCD2

There are 14 intermolecular HBs in this inclusion complex (Table 7). The proton acceptors come from the lactonic oxygen (region **I** in Fig. 1 or 5) and methylol (region **V** in Fig. 1 or 5) of the lactonic ring moiety of andro, or from layer **1** or **2** of the CD. The proton donors come from layer **2**, **3** or **4** of the CD, or from the region ***a***, ***b*** or ***g***. There are

Table 7 The bond path length (BPL, in Å), electron density ρ and Laplacian $\nabla^2\rho$ of the bond critical points for intermolecular hydrogen bonds in the inclusion complex andro:βCD2

X	HB (BCP)	BPL	ρ	$\nabla^2\rho$	PPA	PPD
C151	H173···O21	2.834	0.005	0.019	**2**	***a***(C)
O155	H175···O28	2.387	0.011	0.038	**2**	***b***(O)
C154	H177···O42	2.516	0.009	0.027	**2**	***c***(C)
C159	H181···O42	2.989	0.004	0.015	**2**	***g***(C)
C159	H181···O52	2.720	0.008	0.028	**1**	***g***(C)
C159	H182···O53	2.842	0.006	0.021	**1**	***g***(C)
C151	H173···O67	2.562	0.009	0.029	**4**	***a***(C)
C45	H80···O149	2.284	0.014	0.041	**III**	**2**(C)
O51	H85···O149	2.466	0.009	0.039	**III**	**4**(O)
O55	H95···O149	2.335	0.011	0.036	**III**	**4**(O)
C26	H108···O155	2.305	0.015	0.040	**II**	**2**(C)
C10	H130···O150	2.614	0.007	0.024	**I**	**3**(C)
O71	H135···O150	2.350	0.011	0.037	**I**	**4**(O)
C3	H140···O149	2.689	0.006	0.019	**I**	**3**(C)

PPA and PPD: see the footnote of Table 4

four typical HBs with proton donors connecting with oxygen atoms. The proton donors of the remaining 10 HBs involve with less electronegative carbon atoms. Hence, these are the weaker HBs.

Andro:βCD1 and andro:βCD2 are isomeric inclusion complexes. Their different number of HBs and different topologies reveal a difference of stabilities. Andro:βCD1 is more stable, has more intermolecular HBs (see Table 3 and electronic supplementary material) with more appropriate topology. Thus it causes more significant modification of properties (mainly water solubility) of andro.

Intermolecular HBs in andro:γCD1 and in andro:γCD2

These two inclusion complexes are isomers. There are eight intermolecular HBs in andro:γCD1 (Table 8) and 13

Table 8 The bond path length (BPL, in Å), electron density ρ and Laplacian $\nabla^2\rho$ of the bond critical points for intermolecular hydrogen bonds in the inclusion complex andro:γCD1

X	HB (BCP)	BPL	ρ	$\nabla^2\rho$	PPA	PPD
C169	H199···O26	2.247	0.013	0.041	**4**	***e***(O)
C172	H201···O44	2.302	0.016	0.042	**4**	***g***(C)
C178	H207···O45	3.036	0.003	0.013	**2**	***d***(C)
C179	H210···O45	3.162	0.002	0.011	**2**	***d***(C)
C50	H102···O174	2.734	0.006	0.022	**V**	**3**(C)
C14	H152···O169	2.361	0.013	0.035	**IV**	**3**(C)
O8	H159···O169	2.107	0.018	0.054	**IV**	**4**(O)
O55	H99···O174	2.206	0.019	0.078	**V**	**4**(O)

PPA and PPD: see the footnote of Table 4

Table 9 The bond path length (BPL, in Å), electron density ρ and Laplacian $\nabla^2\rho$ of the bond critical points for intermolecular hydrogen bonds in the inclusion complex andro:γCD2

X	HB (BCP)	BPL	ρ	$\nabla^2\rho$	PPA	PPD
C189	H202···O9	2.557	0.009	0.028	**2**	***g***(C)
C170	H195···O44	2.329	0.014	0.041	**4**	***a***(C)
C170	H195···O55	2.755	0.006	0.024	**4**	***a***(C)
C170	H194···O66	2.412	0.010	0.034	**4**	***a***(C)
C175	H197···O77	2.120	0.018	0.053	**4**	***b***(O)
C189	H203···O86	2.707	0.007	0.023	**1**	***g***(C)
C61	H112···O175	2.542	0.009	0.028	**II**	**3**(C)
O35	H129···O169	2.246	0.013	0.042	**I**	**4**(O)
C32	H132···O174	3.388	0.001	0.006	**III**	**3**(C)
O26	H139···O174	2.313	0.014	0.050	**III**	**4**(O)
C37	H142···O174	2.344	0.011	0.037	**III**	**3**(C)
O17	H149···O174	2.272	0.012	0.040	**III**	**4**(O)
C14	H152···O174	3.110	0.003	0.012	**III**	**3**(C)

PPA and PPD: see the footnote of Table 4

HBs in andro:γCD2 (Table 9). Based on the number of HBs, andro:γCD2 may be more stable than andro:γCD1. However, among the 13 HBs in andro:γCD2, five proton acceptors are associated with one carbonyl oxygen, O174 (region **III** in Figs. 1, 5), i.e. forming a multi-ramified intermolecular HB. This multi-ramified intermolecular HB makes a contribution to the stability of the inclusion complex as one typical HB. Hence, the number of HBs in andro:γCD2 is quite similar to that of andro:γCD1. Moreover, HBs H195···O44 and H195···O45 share the same proton donors in andro:γCD2. These two HBs can be regarded as a "bifurcated". So, the stabilities of the two inclusion complexes are similar. This conclusion is consistent to the ΔEs (-11.2 kcal mol^{-1} for andro:γCD1 and -9.4 kcal mol^{-1} for andro:γCD2).

Through the aforementioned topological analysis, we can reach a conclusion that andro:βCD1 is the most stable and most structurely appropriate among the six 1:1 inclusion complexes. This conclusion can be confirmed by considering the total numbers of HBs or total numbers of intermolecular HBs (Table 3) in the inclusion complexes. Andro:βCD1 has the most total number of HBs (71) and the most intermolecular HBs (14), even though it does not have the most BCPs.

Conclusions

In this work, we carried out DFT and AM1 optimizations on four "monomer" molecules (andro, α, β and γCD) and six 1:1 andro:CD inclusion complexes formed by the monomers. AIM theory was applied to carry out the topological analyses of the six inclusion complexes. We conclude that: (1) The ΔE of andro:βCD1 is the lowest. So, it is the most stable among the six inclusion complexes; (2) Andro:βCD1 also has more HBs and more intermolecular HBs than any other complex; (3) Analyses of topological structures show that the andro:βCD1 complex adopts the most appropriate chelate mode between andro and CD: CD uses its hydrophobic moiety (midsection inside the cavity) to form HBs with andro, while its hydrophilic parts (the top and the bottom of the cone) are preserved for increasing the solubility in aqueous solution. Therefore, our calculations show that βCD is the best conveyer of andro, as has been found experimentally.

Acknowledgments This work was fully supported by a Strategic Research Grant from the City University of Hong Kong (Project No. 7002109). Financial supports for the purchase of a computational device from the Innovation and Technology Fund (Project No. GHP/070/05) of Hong Kong Government is also acknowledged. The authors would also like to express their gratitude to Dr N.B. Wong for his advice and support on the calculation part of this work.

References

1. Fujita T, Takeda Y, Takaishi Y, Yamada T, Kido M, Miura I (1984) Chem Pharm Bull (Tokyo) 32:2117
2. Sheeja K, Guruvayoorappan C, Kuttan G (2007) Int Immunopharmacol 7:211. doi:10.1016/j.intimp.2006.10.002
3. Hebtemariam S (1998) Phytother Res 12:37. doi :10.1002/(SICI)1099-1573(19980201)12:1<37::AID-PTR186>3.0.CO;2-N
4. Puri A, Saxena R, Saxena RP, Saxena KC, Srivastava V, Tandon JS (1993) J Nat Prod 56:995. doi:10.1021/np50097a002
5. Jada SR, Subur GS, Matthews C, Hamzah AS, Lajis NH, Saad MS et al (2007) Phytochemistry 68:904. doi:10.1016/j.phytochem.2006.11.031
6. Maiti K, Mukherjee K, Gantait A, Saha BP, Mukherjee PK (2006) J Pharm Pharmacol 58:1227. doi:10.1211/jpp.58.9.0009
7. Xu Y, Chen A, Fry S, Barrow RA, Marshall RL, Mukkur TKS (2007) Int Immunopharmacol 7:515. doi:10.1016/j.intimp.2006.12.008
8. Cheung HY, Cheung SH, Li JL, Cheung CS, Lai WP, Fong WF, Leung FM (2005) Planta Med 71:1106. doi:10.1055/s-2005-873128
9. Li JL, Cheung HY, Zhang ZQ, Chan GKL, Fong WF (2007) Eur J Pharmacol 568:31. doi:10.1016/j.ejphar.2007.04.027
10. Sheeja K, Kuttan G (2007) Immunopharmacol Immunotoxicol 29:81. doi:10.1080/08923970701282726
11. Zhao DY, Liao KJ, Ma XY, Yan XH (2002) J Incl Phenom 43:259. doi:10.1023/A:1021223407297
12. Ma XY, Liao ZX, Zhaong YL, Chen YZ (2000) J Incl Phenom 36:335. doi:10.1023/A:1008199827029
13. Szejtli J (1998) Chem Rev 98:1743. doi:10.1021/cr970022c
14. Uekama K, Hirayama F, Lrie T (1998) Chem Rev 98:2045. doi:10.1021/cr970025p
15. Goodsell DS, Olson AJ (1990) Proteins: Struc Funct Genet 8:195. doi:10.1002/prot.340080302
16. Morris GM, Goodsell DS, Hury R, Olson AJ (1996) J Comput Aided Mol Des 10:293. doi:10.1007/BF00124499
17. Morris GM, Goodsell DS, Halliday RS, Hury R, Hart WE, Belew RK et al (1998) J Comput Chem 19:1639. doi :10.1002/(SICI)1096-987X(19981115)19:14<1639::AID-JCC10>3.0.CO;2-B

18. Dewar MJS, Zoebisch EG, Healy EF, Stewart JJP (1985) J Am Chem Soc 107:3902. doi:10.1021/ja00299a024
19. Dewar MJS, Jie CX, Yu JG (1993) Tetrahedron 49:5003. doi:10.1016/S0040-4020(01)81868-8
20. Freire RO, Rocha GB, Simas AM (2005) Inorg Chem 44:3299. doi:10.1021/ic048530+
21. Rocha GB, Freire RO, Simas AM, Stewart JP (2006) J Comput Chem 27:1101. doi:10.1002/jcc.20425
22. Frisch MJ, Trucks GW, Schlegel HB, Scuseria GE, Robb MA, Cheeseman JR et al (2003) GAUSSIAN 03 (revision B05). Gaussian Inc, Pittsburgh
23. Popelier PLA (2001) Theor Chem Acc 105:393. doi:10.1007/s002140000224
24. Schwinger J (1981) Phys Rev A 24:2353. doi:10.1103/PhysRevA.24.2353
25. Becke AD (1982) J Chem Phys 76:6037. doi:10.1063/1.442958
26. Bader RFW (1990) Atoms in molecules: a quantum theory. Clarendon Press, Oxford
27. Popelier PLA, Aicken FM, O'Brien SE (2000) In: Hinchliffe A (ed) Chemical modelling: applications and theory, vol 1. The Royal Society of Chemistry, Cambridge, 143 pp
28. Kosov DS, Popelier PLA (2000) J Phys Chem A 104:7339. doi:10.1021/jp0003407
29. Cioslowski J, Mixon ST (1991) J Am Chem Soc 113:4142. doi:10.1021/ja00011a014
30. Ángyán JG, Loos M, Mayer I (1991) J Phys Chem 98:5244. doi:10.1021/j100071a013
31. Fradera X, Austen MA, Bader RFW (1999) J Phys Chem A 103:304. doi:10.1021/jp983362q
32. Popelier PLA (1996) Mol Phys 87:1169. doi:10.1080/00268979650027072
33. Angyan JG, Jansen G, Loos M, Haettig C, Hess BA (1994) Chem Phys Lett 219:267. doi:10.1016/0009-2614(94)87056-X
34. Koch U, Popelier PLA (1995) J Phys Chem 99:9747. doi:10.1021/j100024a016
35. Biegler-Künig F, Schünbohm J, Derdau R, Bayles D, Bader RFW (2000) AIM 2000 version 2.0. McMaster University, Hamilton
36. Stuenkel CA, Dudley RE, Yen SS (1991) J Clin Endocrinol Metab 72:1054
37. Roberts WJ (2003) US Pat Appl Publ, 10 pp, US 2003134831 A1 20030717
38. Zhao DY, Yang SH, Hu M, Ma XY (2003) Chin Chem Lett 14:155
39. Khomutov SM, Sidorov IA, Dovbnya DV, Donova MV (2002) J Pharm Pharmacol 54:617. doi:10.1211/0022357021778925
40. Singer Y, Shity H, Bar R (1991) Appl Microbiol Biotechnol 35:731. doi:10.1007/BF00169886
41. Torricelli C, Martini A, Muggetti L, De Ponti R (1991) Int J Pharm 71:19. doi:10.1016/0378-5173(91)90063-T